Organometallics **1993**, *12*, 4623-4632

On Heterocyclic Systems Containing Lead. 4.[1] Paths to and between Cyclic Diorganotin and -lead Sulfides $[R_2(Sn/Pb)S]_{2,3}$[†]

Otmar R. Flöck and Martin Dräger*

Institut für Anorganische Chemie und Analytische Chemie der Johannes Gutenberg-Universität, D-55099 Mainz, Germany

Received May 24, 1993[®]

Organolead and -tin sulfides were prepared by reaction of difunctionalized organometallic compounds of the form R_2MX_2 (M = Sn, Pb; R = organyl; X = halogen, acetate) and H_2S. Redistribution experiments were conducted, and the exchange of ring segments was confirmed by ^{119}Sn and ^{207}Pb NMR spectroscopy and by mass spectrometry in and from $CDCl_3$ solution. Redistribution of six-membered heterocyclic systems resulted in purely six-membered redistribution species, while redistribution of four- and six-membered heterocycles yielded four-membered redistribution species as well. During the synthesis of $[(cHex)_2SnS]_3$ it was possible to intercept the equivalent of a reaction intermediate in which sulfur is partially replaced by oxygen. By X-ray structure analysis this was assigned to be $Sn_4(cHex)_8Cl_2O_2(SH)_2$, which possesses a fully planar ladderlike central core of ten atoms where the tin atoms acquire five-coordination. On the basis of the structure of this intermediate equivalent species and on the basis of signals assigned to M_4 redistribution species which occurred in all possible combinations (Sn_4, Sn_3Pb, Sn_2Pb_2, $SnPb_3$, Pb_4) in the FD mass spectrometrical measurements, steps in the mechanisms of the electron-donor-catalyzed synthesis of the pure heterocycles and of the redistribution reactions are suggested.

Introduction

Organometallic compounds of lead and tin of the forms R_3MX and R_2MX_2 are used in a wide range of applications. As a consequence of these applications the heavy-metal compounds are released into the environment deliberately (agricultural use and use as antifouling paints) and involuntarily (use as catalysts and stabilizers). Having been set free, these chemicals can react with chalcogen compounds, including OH^-, SH^-, and S^{2-}, to form oligomeric oxides and sulfides of the form $[R_2M^{IV}(O/S)]_n$ (n being a small integer). They then undergo global distribution which is promoted by various processes. One of these processes is believed to involve the redistribution reactions studied in this paper.[2]

According to Skinner[3,4] and Lockhart[5] reactions are defined as redistribution reactions if the position of bonds alone is changed but not their formal character or quantity:

$$A{-}X{-}A + B{-}X{-}B \rightarrow A{-}X{-}B + B{-}X{-}A$$

A and B are organic or inorganic substituents, and X is a central atom or atom group (Moedritzer's[6] "central moiety"). To the best of our knowledge, the mechanism of these reactions has not been clearly disclosed as yet. The aim of this paper is to contribute to the solving of questions concerning the mechanisms of the formation of the pure four- and six-membered heterocyclic starting materials of the redistributions investigated and of the redistributions themselves. In an earlier paper[1] we discussed a system similar to those addressed here; studies are continued in this work. Older work of this kind has been detailed in a review by Wrackmeyer.[7]

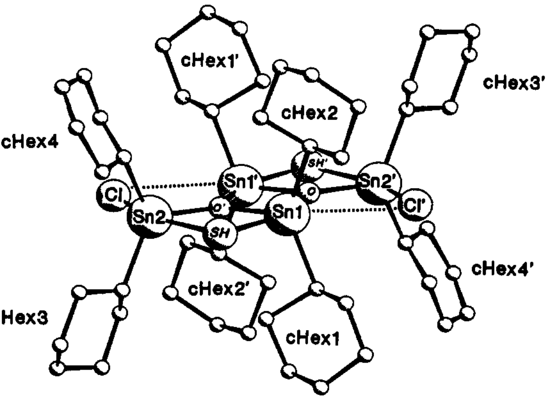

Figure 1. Molecule 1 of $Sn_4(cHex)_8Cl_2O_2(SH)_2$ with a mean labeling for both molecules (cf. Table VII). Molecule 2 looks alike. The groups cHex3 in molecule 2 and cHex4 in both molecules are slightly disordered. Ortep plots of both molecules with full labeling are confusing.

Table I. Pb and Sn NMR Chemical Shifts (ppm[a]) of $[R_2M^{IV}S]_2$ (M^{IV} = Sn, Pb) and $[(tBu)_2SnS]_2$

	organic substituents R					
	trimeric					dimeric
M^{IV}	Ph	oTol	mTol	pTol	cHex	tBu
Pb	172.8	172.5		180.4		
Sn	15.0	12.8	17.7	19.3	92.0	124.2[b]

[a] Conditions: references $SnMe_4$ and $PbMe_4$; solvent $CDCl_3$; $[(oTol)_2SnS]_3$ in benzene-d_6, δ 14.0 ppm. [b] 124.0 ppm.[20]

[†] Dedicated to Prof. Dr. Heinrich Nöth, on the occasion of his 65th birthday.

[®] Abstract published in *Advance ACS Abstracts*, October 15, 1993.

(1) Part 3: Schmidt, B. M.; Dräger, M. *J. Organomet. Chem.* **1990**, *399*, 63.

(2) Craig, P. J. *Organometallic Compounds in the Environment*; Longman: Harlow, U. K., 1986.

(3) Skinner, H. A.; Tees, T. F. S. *J. Chem. Soc.* **1953**, 3378.

(4) Skinner, H. A. *Recl. Trav. Chim. Pays-Bas* **1954**, *73*, 991.

(5) Lockhart, J. C. *Redistribution Reactions*; Academic Press: New York, London, 1970.

(6) Moedritzer, K.; Considine, W. J. Redistribution Reactions in Chemistry. *Ann. N.Y. Acad. Sci.* **1969**, *159*, 1.

0276-7333/93/2312-4623$04.00/0

Table II. Geometric Data (Esd's in Parentheses) for the Planar Central Cores of the Two Independent Centrosymmetric Molecules of $Sn_4(cHex)_8Cl_2O_2(SH)_2$

atom[a]	molecule 1	molecule 2	atom[a]	molecule 1	molecule 2
Bond Lengths (Å)[b]					
Sn1–SH	2.665(7)	2.667(7)	Sn2–SH	2.813(7)	2.818(8)
Sn1–O	2.15(2)	2.15(2)	Sn2–Cl	2.441(8)	2.427(9)
Sn1–O′	2.07(2)	2.06(2)	Sn2–O′	2.01(2)	2.02(2)
Sn1–cHex1	2.15(2)	2.13(3)	Sn2–cHex3	2.16(3)	2.17(3)
Sn1–cHex2	2.17(2)	2.13(3)	Sn2–cHex4	2.15(3)	2.18(3)
Sn1–Cl′	[3.391(8)	3.474(9)]			
Bond Angles (deg) of the Coordination Polyhedra around the Atoms Sn1[c] and Sn2					
SH–Sn1–O	153.5(6)	154.0(5)	SH–Sn2–Cl	162.3(2)	164.8(3)
SH–Sn1–O′	78.2(6)	79.4(5)	SH–Sn2–O′	75.6(7)	76.3(5)
SH–Sn1–cHex1	92.7(7)	91.8(7)	SH–Sn2–cHex3	87.7(8)	86.4(8)
SH–Sn1–cHex2	94.6(7)	94.3(8)	SH–Sn2–cHex4	89.3(9)	84.5(9)
SH–Sn1–Cl′	[143.8(2)]	[144.0(2)]			
O–Sn1–O′	75.3(9)	74.6(7)	Cl–Sn2–O′	86.8(7)	88.4(5)
O–Sn1–cHex1	97.0(8)	98.0(8)	Cl–Sn2–cHex3	100.6(8)	100.2(8)
O–Sn1–cHex2	94.0(8)	94.9(8)	Cl–Sn2–cHex4	97.8(9)	101.0(9)
O–Sn1–Cl′	[62.7(5)]	[62.1(5)]			
O′–Sn1–cHex1	110.1(8)	110.6(9)	O′–Sn2–cHex3	114.9(10)	113.7(9)
O′–Sn1–cHex2	110.5(8)	112.5(9)	O′–Sn2–cHex4	114.9(10)	111.2(10)
O′–Sn1–Cl′	[138.1(6)]	[136.6(5)]			
cHex1–Sn1–cHex2	139.4(9)	136.9(11)	cHex3–Sn2–cHex4	127.5(12)	130.4(11)
cHex1–Sn1–Cl′	[76.5(7)]	[75.7(8)]			
cHex2–Sn1–Cl′	[74.2(7)]	[74.6(8)]			
Bond Angles (deg) at the Atoms O, SH, and Cl of the Four-Membered Rings					
Sn1–O′–Sn1′	104.7(9)	105.4(7)	Sn1–SH–Sn2	82.2(2)	81.4(2)
Sn1–O′–Sn2	131.3(8)	131.6(7)	Sn2–Cl–Sn1′	[79.2(2)	77.9(3)]
Sn2–O′–Sn1′	124.1(8)	122.9(7)			
Σ	360.1	359.9			
Least-Squares Planes Averaging the Ten Atoms of the Central Core (Deviation (Å))					
figure of merit	6.0	20.1			
mean dev	±0.007(7)	±0.009(7)			
max dev	±0.009(2) (Sn1)	±0.025(15)(O)			
dev (C_{ipso} of cHex)	±1.98(3)	±1.98(3)			

[a] Atom identifications as given in Figure 1 and Table VII. [b] Shortest intermolecular Sn···Cl contact 4.880(8) Å. There are no short intermolecular contacts between SH groups (hydrogen bonds) or to/between Cl and O. [c] Ten angles by "trigonal bipyramidal" five-coordination; the five additional angles for the questionable "octahedral" six-coordination are in brackets.

Results

Starting Material. Trimeric diorganolead sulfides and analogous trimeric and dimeric tin compounds prepared by treatment of the corresponding dihalogenides or diacetates with hydrogen sulfide in dry toluene comprise the starting materials for redistribution experiments. They are summarized in Table I, together with their ^{119}Sn and ^{207}Pb NMR chemical shifts.

When the reaction of $(cHex)_2SnCl_2$ and H_2S was carried out in moist toluene and under slightly basic conditions, it was possible to intercept $Sn_4(cHex)_8Cl_2O_2(SH)_2$, the equivalent of the reaction intermediate $Sn_4(cHex)_8Cl_2S_2(SH)_2$. The latter underwent rearrangement, yielding the heterocyclic product $[(cHex)_2SnS]_3$, first mentioned in ref 8. This product is fully stable against hydrolysis.

The crystal structure of $Sn_4(cHex)_8Cl_2O_2(SH)_2$ contains two centrosymmetric molecules which are identical within the range of standard deviation but which are crystallographically independent. Figure 1 shows molecule 1 with a mean labeling for both molecules (cf. Table VII), and Table II quantitatively describes the central cores of both molecules. These cores form fully planar, centrosymmetric, ladderlike arrays of $Cl_2Sn_4O_2(SH)_2$ in which the Sn atoms acquire five-coordination. Further expansion to six-coordination of Sn1 (broken line in Figure 1) is questionable. It should be mentioned that it cannot be excluded by X-ray reasoning alone that the position of SH is occupied by Cl and vice versa.

Scheme I[a]

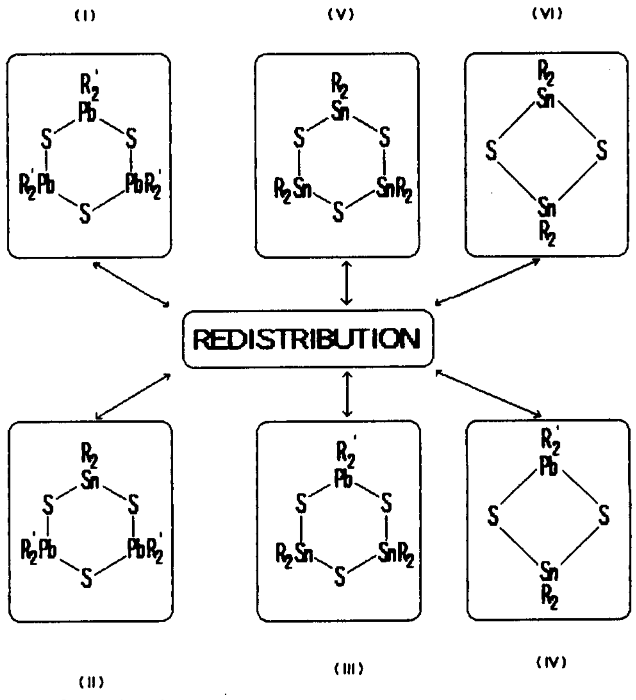

[a] R bound to Sn: Ph, oTol, pTol, mTol, cHex, tBu. R′ bound to Pb: Ph, oTol, pTol.

Exchange Experiments. Redistribution experiments were conducted with the pure lead and tin heterocycles listed in Table I. Scheme I shows the redistribution species

---

(7) Wrackmeyer, B. *Annu. Rep. NMR Spectrosc.* **1985**, *16*, 73.

(8) Jung, Ok Sang; Kim, Min Jung; Jeong, Jong Hwa; Sohn, Youn Soo. *Bull. Korean Chem. Soc.* **1989**, *10*(4), 343.

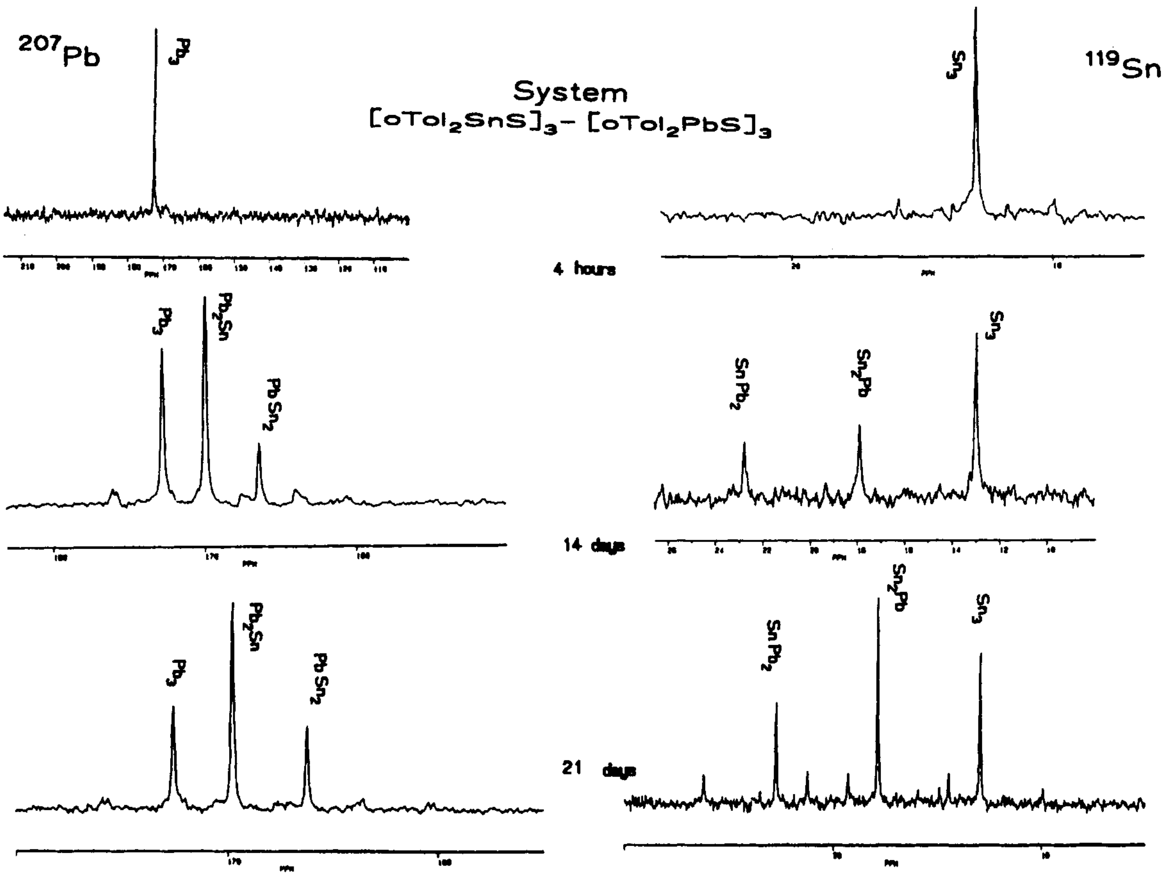

Figure 2. Time dependency of equilibration of the system [$(oTol)_2SnS]_3$–]$(oTol)_2PbS]_3$ traced by ^{207}Pb and ^{119}Sn NMR.

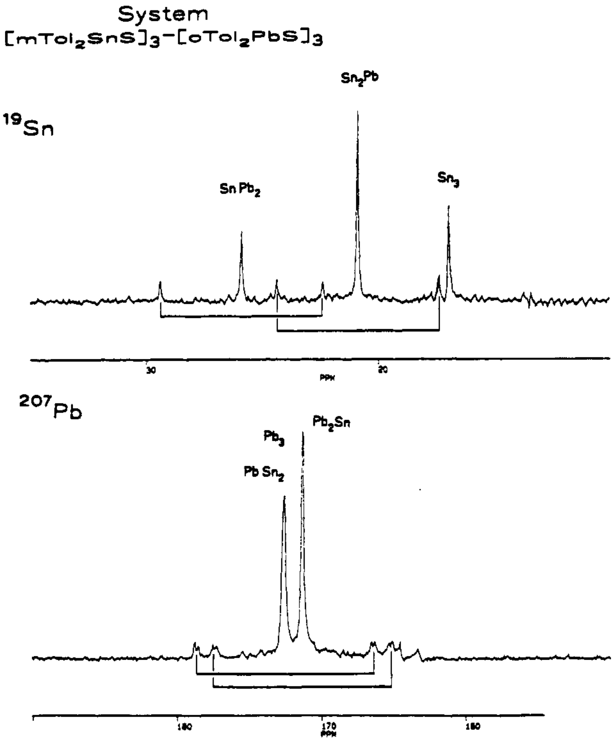

Figure 3. ^{119}Sn and ^{207}Pb NMR spectra of the system [$(mTol)_2SnS]_3$–[$(oTol)_2PbS]_3$ depicting the degeneracy of ^{207}Pb signals for the species [$(oTol_2PbS]_3$ and [$(mTol)_2SnS]_2$-[$(oTol)_2PbS$].

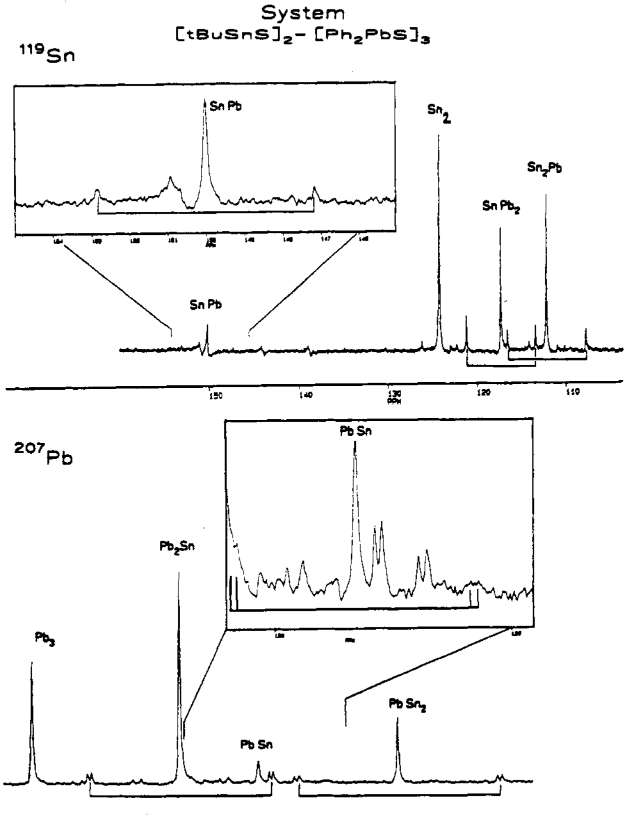

Figure 4. ^{119}Sn and ^{207}Pb NMR spectra of the system [$(tBu)_2SnS]_2$–[$Ph_2PbS]_3$, exemplary of the studied four-/six-membered heterocyclic exchange systems (mixed four-membered-ring signals given as insets).

which occurred, three heterocycles containing only one sort of metal atom and three being mixed-metal systems.

Redistribution Experiments Followed by NMR Spectroscopy. In addition to the expected signals from the starting materials, resonance lines appeared that indicated the presence of redistribution products (cf. Figures 2–4). In solution, the metallic atoms of one sort

Table III. Chemical Shifts (ppm) and Coupling Constants (Hz) for the Redistribution Species

components	$\delta(^{207}Pb)$	$\delta(^{119}Sn)$	^{207}Pb NMR $^2J(^{207}Pb–S–^{119}Sn/^{117}Sn)$		^{119}Sn NMR $^2J(^{119}Sn–S–^{207}Pb/^{119}Sn)^b$	
$[Ph_2PbS]_3$ (I)	173.3[c]					
$[Ph_2PbS]_2Pb_2SnS^d$ (II)	170.5	25.8	227.3	216.6	226.2	
$Ph_2PbS[Ph_2SnS]_2^d$ (III)	166.8	20.9	225.2	216.6	225.7	201.9
$[Ph_2SnS]_3^d$ (V)		15.8				205.2
$[Ph_2PbS]_2(pTol)_2SnS$ (II)	168.6	29.9	226.9	216.7	227.3	
$Ph_2PbS[(pTol)_2SnS]_2$ (III)	163.2	24.6	228.9	218.7	228.9	*a*
$[(pTol)_2SnS]_3$ (V)		19.3				*a*
$[Ph_2PbS]_2(oTol)_2SnS$ (II)	166.6	24.8	227.3	217.3	227.4	
$Ph_2PbS[(oTol)_2SnS]_2$ (III)	161.5	18.2	224.7	214.7	224.8	186.1
$[(oTol)_2SnS]_3$ (V)		13.0				196.8
$[Ph_2PbS]_2(mTol)_2SnS$ (II)	169.4	26.7	227.9	217.6	227.1	
$Ph_2PbS[(mTol)_2SnS]_2$ (III)	164.9	21.9	225.8	216.9	226.8	197.0
$[(mTol)_2SnS]_3$ (V)		16.9				201.8
$[Ph_2PbS]_2(cHex)_2SnS$ (II)	161.3	103.0	234.3	225.5	232.1	
$Ph_2PbS[(cHex)_2SnS]_2$ (III)	154.4	98.9	236.1	225.3	237.2	146.5
$[(cHex)_2SnS]_3$ (V)		92.1				155.2
$[Ph_2PbS]_2(tBu)_2SnS$ (II)	162.4	117.2	230.7	220.7	231.1	
$Ph_2PbS[(tBu)_2SnS]_2$ (III)	146.1	112.1	262.2	250.5	262.1	124.5
$Ph_2PbS(tBu)_2SnS$ (IV)	156.7	150.0	172.7	162.5	170.1	
$[tBu_2SnS]_2$ (VI)		124.1				120.7
$[(pTol)_2PhS]_3$ (I)	180.8[c]					
$[(pTol)_2PbS]_2(pTol)_2SnS$ (II)	178.1	29.2	220.9	211.1	222.3	
$(pTol)_2PbS[(pTol)_2SnS]_2$ (III)	174.8	24.4	221.9	211.9	223.2	199.3
$[(pTol)_2SnS]_3$ (V)		19.4				201.7
$[(pTol)_2PbS]_2(oTol)_2SnS$ (II)	176.4	23.4	*a*	*a*	223.7	
$(pTol)_2PbS[(oTol)_2SnS]_2$ (III)	172.8	17.7	*a*	*a*	218.4	188.4
$[(oTol)_2SnS]_3$ (V)		13.0				186.7
$[(pTol)_2PbS]_2(mTol)_2SnS$ (II)	179.1	26.1	221.9	210.8	221.9	
$(pTol)_2PbS[(mTol)_2SnS]_2$ (III)	176.5	21.4	221.8	212.1	221.1	198.5
$[(mTol)_2SnS]_3$ (V)		17.0				200.7
$[(pTol)_2PbS]_2(cHex)_2SnS$ (II)	171.3	102.3	225.5	216.2	228.2	
$(pTol)_2PbS[(cHex)_2SnS]_2$ (III)	164.5	98.4	230.6	219.7	231.2	148.6
$[(cHex)_2SnS]_3$ (V)		92.1				154.9
$[(pTol)_2PbS]_2(tBu)_2SnS$ (II)	171.9	117.4	225.5	215.6	225.6	
$(pTol)_2PbS[(tBu)_2SnS]_2$ (III)	155.5	112.0	257.5	245.2	257.4	121.9
$(pTol)_2PbS(tBu)_2SnS$ (IV)	171.1	149.8	*a*	*a*	171.9	
$[(tBu)_2SnS]_2$ (VI)		124.1				121.1
$[(oTol)_2PbS]_3$ (I)	172.6[c]					
$[(oTol)_2PbS]_2(pTol)_2SnS$ (II)	169.9	29.1	209.2	200.2	209.0	
$(oTol)_2PbS[(pTol)_2SnS]_2$ (III)	169.0	23.8	212.0	201.7	212.2	198.0
$[(pTol)_2SnS]_3$ (V)		19.4				202.1
$[(oTol)_2PbS]_2(oTol)_2SnS$ (II)	169.7	22.8	206.0	197.2	206.4	
$(oTol)_2PbS[(oTol)_2SnS]_2$ (III)	166.2	17.9	202.2	193.3	202.9	184.6
$[(oTol)_2SnS]_3$ (V)		13.0				187.0
$[(oTol)_2PbS]_2(mTol)_2SnS$ (II)	171.3	25.9	208.0	198.3	209.3	
$(oTol)_2PbS[(mTol)_2SnS]_2$ (III)	172.6	20.9	209.2	200.2	209.7	198.1
$[(mTol)_2SnS]_3$ (V)		16.4				200.8
$[(oTol)_2PbS]_2(cHex)_2SnS$ (II)	162.3	100.1	219.5	209.5	219.8	
$(oTol)_2PbS[(cHex)_2SnS]_2$ (III)	155.7	97.1	234.1	223.4	233.8	138.1
$[(cHex)_2SnS]_3$ (V)		92.1				*a*
$[(oTol)_2PbS]_2(tBu)_2SnS$ (II)	159.4	114.2	221.8	210.9	222.2	
$(oTol)_2PbS[(tBu)_2SnS]_2$ (III)	141.1	109.2	269.9	257.2	269.5	*a*
$(oTol)_2PbS(tBu)_2SnS$ (IV)	163.8	151.2	*a*	*a*	173.0	
$[(tBu)_2SnS]_2$ (VI)		124.1				121.4

[a] Not observed. [b] $^2J(^{119}Sn–S–^{119}Sn) = {}^2J(^{117}Sn–S–^{119}Sn) \times 1.0465$. [c] Average of all measurements on redistribution systems where this compound is involved. [d] Data from ref 1.

within each molecule of Scheme I are chemically equivalent and therefore responsible for only one peak in the ^{119}Sn and ^{207}Pb NMR spectra. Intermolecularly, however, lead atoms in I–IV as well as tin atoms in II–VI are chemically inequivalent, so that the chemical shift caused by heavy atoms of a certain redistribution species is different from those created by the heavy atoms of a different redistribution species. This is the reason as many resonance signals as redistribution species carrying the investigated metal atom (one less than the sum of all the redistribution species) could be identified (degeneracy of two signals in the ^{207}Pb part of Figure 3). Table III presents the NMR data observed in the systems investigated.

Chemical shifts of signals caused by pure organolead and -tin sulfur heterocycles in redistribution solution deviated from those produced by the same substances in pure solution only up to +0.6 ppm in the case of ^{207}Pb NMR measurements and between −1.3 and +0.2 ppm in the case of ^{119}Sn NMR examinations. Considering the influence of tiny deviations in concentration and temperature and taking into account the digital resolution of 0.5 Hz, these values were within the margin of error and will not be discussed further.

In the ^{207}Pb NMR spectra the increasing share of organotin segments in the redistribution species (caused by the exchange of organometal segments) resulted in a shift of the resonance line of the observed redistribution species to higher fields. In the ^{119}Sn NMR studies a low-field shift is observed with an increasing share of organolead units. These observations have also been found in earlier studies.[1]

If measurements are carried out for a sufficient period, coupling satellites $^2J(^{207}\mathrm{Pb{-}S{-}}^{119/117}\mathrm{Sn})$ could be observed in the ^{207}Pb NMR spectra, and coupling satellites $^2J(^{119}\mathrm{Sn{-}S{-}}^{207}\mathrm{Pb})$ in the corresponding ^{119}Sn NMR spectra reaffirm those from the ^{207}Pb studies. In addition, $^2J(^{207}\mathrm{Pb{-}S{-}}^{119}\mathrm{Sn})$ coupling constants can be calculated from $^2J(^{207}\mathrm{Pb{-}S{-}}^{117}\mathrm{Sn})$ couplings by multiplication by 1.0465: the calculated coupling constants deviate only slightly from those observed. Furthermore, satellites of weaker intensity assigned to $^2J(^{119}\mathrm{Sn{-}S{-}}^{117}\mathrm{Sn})$ couplings appeared in the ^{119}Sn NMR spectra.

Relative signal intensities were established by determining the heights of the main signals and by mathematically supplementing the intensities flowing into the coupling satellites, taking into account the percent occurrence of the coupling species. In Table IV the relative intensities of the observed signals are listed. The relative intensities of ^{119}Sn and ^{207}Pb NMR signals of the $[(\mathrm{aryl})_2\mathrm{SnS}]_3$–$[(\mathrm{aryl})_2\mathrm{PbS}]_3$ redistribution systems tended to approach the ratios

$$[(\mathrm{aryl})_2\mathrm{SnS}]_3:[(\mathrm{aryl})_2\mathrm{SnS}]_2[(\mathrm{aryl})_2\mathrm{PbS}]:[(\mathrm{aryl})_2\mathrm{SnS}][(\mathrm{aryl})_2\mathrm{PbS}]_2:[(\mathrm{aryl})_2\mathrm{PbS}]_3 = 1:2:1:0 \text{ and } 0:1:2:1$$

This was illustrated vividly by the redistribution system $[(\mathrm{oTol})_2\mathrm{SnS}]_3$–$[(\mathrm{oTol})_2\mathrm{PbS}]_3$, which took 21 days for the steady state of the dynamic redistribution equilibrium (in which constant exchanges of ring segments take place) to be reached (Table IV and Figure 2).

From this ratio of the relative intensities, a ratio of the redistribution species

$$[(\mathrm{aryl})_2\mathrm{SnS}]_3:[(\mathrm{aryl})_2\mathrm{SnS}]_2[(\mathrm{aryl})_2\mathrm{PbS}]:[(\mathrm{aryl})_2\mathrm{SnS}][(\mathrm{aryl})_2\mathrm{PbS}]_2:[(\mathrm{aryl})_2\mathrm{PbS}]_3 = 1:3:3:1$$

can be calculated. This indicates a statistically occurring redistribution. No such tendencies of an establishment of a definite ratio of relative intensities could be observed either in ^{207}Pb NMR measurements or in the ^{119}Sn NMR spectra of the redistribution systems $[(\mathrm{alkyl})_2\mathrm{SnS}]_3$–$[(\mathrm{aryl})_2\mathrm{PbS}]_3$.

Table IV. Relative Signal Intensities of the Redistribution Systems $[\mathrm{R'_2PbS}]_3/[\mathrm{R_2SnS}]_{2,3}$

		rel signal intens[a] (Pb:Sn)					
R′/R	NMR type	Sn only	1:2	1:1	2:1	Pb only	elapsed time
Ph/pTol	Pb		1.70		2.60	1.00	immediately
	Sn	1.00	2.16		1.03		immediately
Ph/oTol	Pb		0.00		0.00	1.00	2 h
	Pb		1.00		2.04	1.10	5 days
	Sn	1.00	0.00		0.00	0.00	2 h
	Sn	1.90	1.45		1.00		1 day
	Sn	1.49	1.85		1.00		5 days
Ph/mTol	Pb		1.33		2.50	1.00	immediately
	Sn	1.08	1.71		1.00		immediately
Ph/cHex	Pb		2.38		3.91	1.00	immediately
	Sn	1.00	3.43		1.61		immediately
Ph/tBu	Pb[b]		1.72	1.00	8.03	6.41	immediately
	Pb		1.61	1.00	5.75	2.75	immediately
	Sn[b]	2.33	1.90	1.00	2.90		immediately
	Sn	4.41	2.61	1.00	2.67		immediately
pTol/pTol	Pb		1.51		2.72	1.00	several hours
	Sn	1.00	2.12		1.09		several hours
pTol/oTol	Pb		0.00		0.00	1.00	4 h
	Pb		1.00		2.33	1.31	7 days
	Sn	3.20	1.00		1.20		2 days
	Sn	1.08	1.73		1.00		7 days
pTol/mTol	Pb		1.00		2.21	1.12	immediately
	Sn	1.00	2.85		1.13		immediately
pTol/cHex	Pb		1.91		3.13	1.00	immediately
	Sn	1.00	3.60		1.89		immediately
pTol/tBu	Pb		1.23	1.00	4.96	3.65	immediately
	Sn	3.69	2.44	1.00	2.38		immediately
oTol/pTol	Pb		1.3		2.33	1.00	immediately
	Sn	1.00	2.43		1.46		immediately
oTol/oTol	Pb		0.00		0.00	1.00	4 h
	Pb		1.00		3.09	2.16	14 days
	Pb		1.00		2.33	1.05	21 days
	Sn	1.00	0.00		0.00		4 h
	Sn	2.35	1.20		1.00		14 days
	Sn	1.21	1.85		1.00		21 days
oTol/mTol	Pb		1.00[c]		~1.1[c]	1.00[c]	immediately
	Sn	1.08	2.40		1.00		immediately
oTol/cHex	Pb		1.00		1.36	2.33	several hours
	Sn	1.00	3.65		1.55		several days
oTol/tBu	Pb		1.19	1.00	3.14	3.63	immediately
	Sn	4.20	2.08	1.00	1.70		immediately

[a] Determined by signal heights; coupling intensities taken into account. [b] Metal ratio (Pb:Sn) 1:1. [c] Degeneracy; "experimental" integration (we thank an unknown reviewer for the hint).

The ^{207}Pb NMR spectrum of the exchange system $[(\mathrm{mTol})_2\mathrm{SnS}]_3$–$[(\mathrm{oTol})_2\mathrm{PbS}]_3$ (Figure 3) exhibited a special characteristic, attributable to degeneracy; there were only two main signals to be seen. Signal assignments were made as follows. The signal occurring at δ 172.6 ppm was attended symmetrically by coupling signals of 209.2 and 200.2 Hz. These were identified as $^2J(^{207}\mathrm{Pb{-}S{-}}^{119/117}\mathrm{Sn})$ coupling constants, because they could be recalculated from each other by multiplication/division by 1.0465, which normally is the case with such coupling constants. The deviation of the theoretical value from that observed is only 0.3 Hz, which was within the accuracy of measurement. If the signal at δ 172.6 ppm resulted from the pure organolead component alone, these coupling constants would not occur. The ratio of the relative intensities of the signals was $I(\delta\ 172.6\ \mathrm{ppm}):I(\delta\ 171.3\ \mathrm{ppm}) \approx 1:1$ (see footnote *c* in Table IV); if the species $\mathrm{Pb_2Sn}$ and $\mathrm{PbSn_2}$ were responsible for the signal at δ 172.6 ppm, this ratio would be 3:1.

In the systems $[(\mathrm{tBu})_2\mathrm{SnS}]_2$–$[(\mathrm{aryl})_2\mathrm{PbS}]_3$, in addition to the three signals representing the six-membered heterocyclic redistribution species and the starting substances, another resonance line could be seen in each ^{119}Sn and ^{207}Pb NMR spectrum (cf. Figure 4), indicating a total of five redistribution species involved in these exchange experiments. In the ^{207}Pb NMR studies, due to a sufficiently long measuring time for the exchange system $[(\mathrm{tBu})_2\mathrm{SnS}]_2$–$[\mathrm{Ph_2PbS}]_3$ this signal was also accompanied symmetrically by two pairs of satellites. The coupling constants could again be recalculated from each other by multiplication/division by 1.0465 and thus were identified as $^2J(^{207}\mathrm{Pb{-}S{-}}^{119/117}\mathrm{Sn})$ satellites. Since the coupling constants found were 60–90 Hz smaller than those found for the systems $\mathrm{Pb_2Sn}$ and $\mathrm{PbSn_2}$, this signal was assigned to the postulated mixed four-membered cyclic systems PbSn. This assignment was confirmed by ^{119}Sn NMR measurements.

In all the redistribution systems involving $[(\mathrm{tBu})_2\mathrm{SnS}]_2$, due to $^2J(^{119}\mathrm{Sn{-}S{-}}^{119}\mathrm{Sn}/^{207}\mathrm{Pb})$ couplings accompanying

Table V. Frequency of Polynuclear Fragments Observed in the Mass Spectrometrical Measurements of the Redistribution Species

system	reflected measuring range (m/e)	signals of fragments carrying x metallic atoms (x = 1–5)[b]
$[Ph_2PbS]_3/[(pTol)_2SnS]_3$	650–1737	3 (12), 4 (12), 5 (1)[a]
$[Ph_2PbS]_3/[oTol)_2SnS]_3$	998–1737	3 (4), 4 (6)
$[Ph_2PbS]_3/[(mTol)_2SnS]_3$	727–1675	3 (13), 4 (12), 5 (1)[a]
$[Ph_2PbS]_3/[(cHex)_2SnS]_3$	813–1462	3 (13), 4 (6)
$[Ph_2PbS]_3/[(tBu)_2SnS]_2$	473–1423	2 (3), 3 (5), 4 (4)
$[(pTol)_2PbS]_3/[(pTol)_2SnS]_3$	905–1801	3 (9), 4 (7), 5 (1)[a]
$[(pTol)_2PbS]_3/[(oTol)_2SnS]_3$	905–1475	3 (3), 4 (2), 5 (1)[a]
$[(pTol)_2PbS]_3/[(mTol)_2SnS]_3$	905–1801	3 (5), 4 (7), 5 (1)[a]
$[(pTol)_2PbS]_3/[(cHex)_2SnS]_3$	705–1477	3 (8), 4 (8)
$[(pTol)_2PbS]_3/[(tBu)_2SnS]_2$	530–1559	2 (1), 3 (6), 4 (5)
$[(oTol)_2PbS]_3/[(pTol)_2SnS]_3$	905–1832	3 (9), 4 (8)
$[(oTol)_2PbS]_3/[(oTol)_2SnS]_3$	905–1385	3 (7), 4 (1)
$[(oTol)_2PbS]_3/[(mTol)_2SnS]_3$	905–1780	3 (10), 4 (11)
$[(oTol)_2PbS]_3/[(cHex)_2SnS]_3$	707–975	3 (4)
$[(oTol)_2PbS]_3/[(tBu)_2SnS]_2$	530–1559	2 (1), 3 (2)

[a] Assignable as well to M_4 units having more organic substituents. [b] Number of different fragments given in parentheses.

the ^{119}Sn NMR signals which were shifted to the most high-field position the latter were assigned to mixed six-membered cyclic redistribution species containing lead and tin in the ratio Pb:Sn = 1:2. In accord with this trend, signals of six-membered species containing two lead and one tin atom were shifted about 5 ppm to a lower field position compared to the initial compound and they were accompanied by $^2J(^{207}Pb–S–^{119}Sn)$ satellites only. The resonance lines of the pure tin compounds (four-membered heterocycles) were shifted approximately 12–15 ppm further to lower field. Shifted to the most low-field position could be found signals that were surrounded by satellites on the order of 170 Hz if the measuring time was sufficiently long. For the redistribution system $[Ph_2PbS]_3–[(tBu)_2SnS]_2$ these couplings were also identified in the accompanying ^{207}Pb NMR investigations and were therefore interpreted as $^2J(^{119}Sn–S–^{207}Pb)$ coupling satellites of a four-membered heterocyclic redistribution species possessing one lead and one tin atom. The signals of four-membered heterocyclic systems were separated (shifted to more lowfield positions) from those arising from six-membered redistribution species.

Redistributions Followed by Mass Spectrometry. All the redistribution solutions were examined by FD mass spectrometry (for details see the Experimental Section). Organyl–metal bonds were found to be prone to cleavage under FD mass spectrometric conditions. This was indicated by the occurrence of signals which were assigned to molecules or fragments containing more, less, or different organic substituents bonded to their metallic atoms than would be expected if destruction and subsequent new formation of such a linkage had not taken place. Since there were also a variety of signals that indicated fragments with metal–metal bindings and fragments with sulfur–sulfur bindings, it was concluded that the metal–sulfur bond is labile as well and can easily be broken and reformed. The mass spectrometric data confirmed the findings obtained through NMR spectroscopy.

Table V summarizes the signals of organometallic compounds observed in the FD mass spectra, their frequency, and their most likely assignment to M_x fragments (M = Pb/Sn; x = 1–5) (for further information see supplementary material). Figure 5 illustrates an example of the mass spectra obtained.

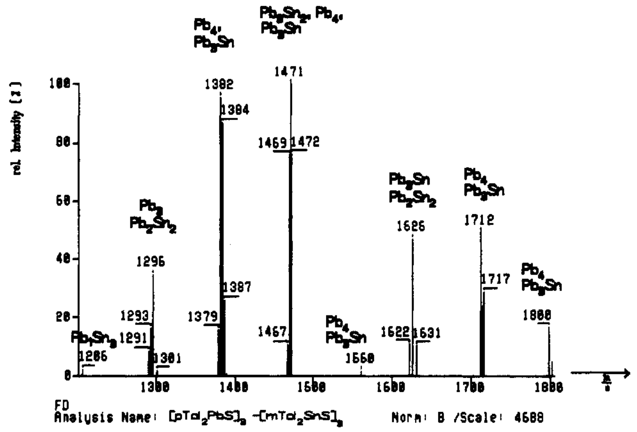

Figure 5. FD mass spectrum of the redistribution system $[(pTol)_2PbS]_3–[(mTol)_2SnS]_3$ (signals assigned to fragments of the most likely metallic species).

Discussion

Syntheses and Synthetic Intermediates. As mentioned before, it was possible to obtain $Sn_4(cHex)_8Cl_2O_2(SH)_2$ in the course of the production of $[(cHex)_2SnS]_3$; once $[(cHex)_2SnS]_3$ is formed, this compound remains stable against hydrolysis. The centrosymmetric ladderlike compound contains five-coordinate tin and three-coordinate oxygen forming its core system. A possible course of reaction steps is pictured in Scheme II.

In collaboration with the auxiliary base NEt_3 electrophilic tin is attacked by nucleophilic HS^- (**1**), causing the formation of a trigonal-bipyramidal transitional state (**2**). The latter decomposes with cleavage of triethylamine-hydrohalogenide, creating the tetrahedral system **3**. With NEt_3 as catalyst, **3** can combine with **1**, expelling HCl and creating a four-membered cyclic unit (**4**) containing four- and five-coordinate tin. **4** rapidly becomes stabilized, decaying into tetramer **6**, which contains five-coordinate tin only, or it reacts with SH^- or OH^- with expulsion of Cl^-, resulting in the four-membered heterocycle **5**. **4** is in equilibrium with tetramer **6**, which is formed as well by dimerization of **5**. If the open circle in Scheme II is sulfur and the dotted circle is SH, **6** decomposes with the liberation of **3** and HCl, creating the six-membered heterocyclic product **7** finally having only four-coordinate tin. Tetramer **6** precipitates if the open circle is oxygen and the dotted circle is SH (created by a formal proton shift); thus, it can be intercepted. **6** also precipitates if created by dimerization of **5** analogues which contain oxygen instead of sulfur (formed by impact of moisture), resulting in an amorphous powder. This causes the calculated and the observed elementary analyses to differ with regard to the sulfur percentage (cf. the Experimental Section). In the course of the syntheses a delay is observed (cf. the Experimental Section), and we therefore conclude the reaction steps between **3**, **4**, and **5** are slow.

In 1961 Reichle[9] postulated a transitional state containing more than four-coordinate tin when he prepared diorganotin–sulfur heterocycles by interaction of R_2SnO compounds with sulfide. Alleston et al.[10] and Reifenberg and Considine[11] report higher coordinated intermediates in the mechanism of the base-catalyzed hydrolysis of diorganotin dihalogens. Due to their lack of X-ray

---

[9] Reichle, W. T. *J. Org. Chem.* **1961**, *26*, 4634.

[10] Alleston, D. L.; Davies, A. G.; Hancock, M.; White, R. F. M. *J. Chem. Soc.* **1963**, 5469.

[11] Reifenberg, G. H.; Considine, W. J. *J. Organomet. Chem.* **1967**, *10*(2), 279.

Scheme II

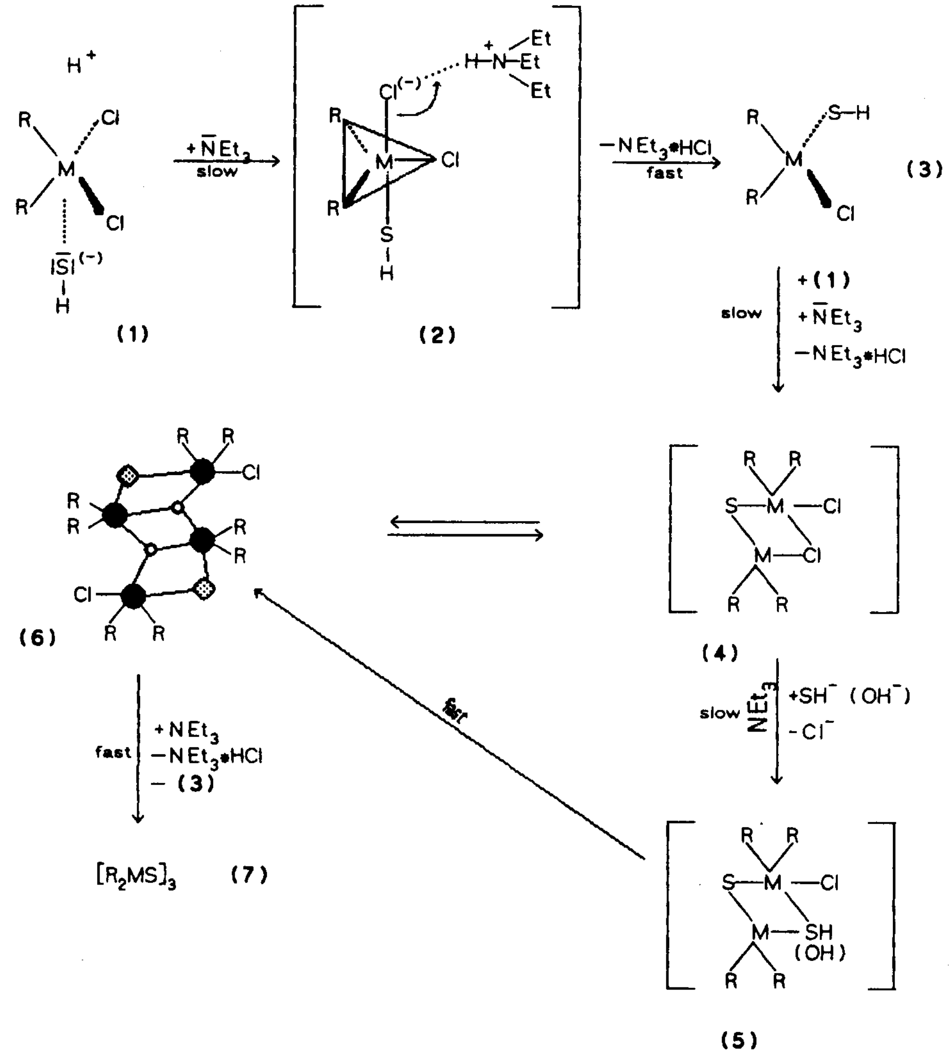

M = ● : tin, lead

A)	◈ :	S	○ :	halogen	labile (equilibrium)
B)		SH		sulfur	reorganizes (⟶ products)
C)		SH		oxygen	stable ("interceptable" single crystals)
D)		OH		oxygen	stable (white powder)

crystallographic data the structure of these intermediate is addressed only vaguely.

Redistributions. Depending on the substituents involved, the time needed to establish the stationary state of the dynamic equilibrium, where constant exchanges of ring segments occur, varied between a few minutes and several weeks. Interactions of electron donors with lead and tin appear to have a major impact on the rate constant for establishment of the steady state of the dynamic equilibrium. These electron donors can be Lewis-basic impurities as well as the sulfur atoms of the heterocycles themselves. Especially in systems involving $[(oTol_2SnS]_3$ an impaired rate of accommodation of the steady state was observed. This may be explained by the hindrance of approximation of the metallic atom and the electron-donating chalcogen induced by steric effects of the *o*-tolyl group.

The creation of new substances (redistribution species) was indicated by the appearance of three and four signals and their attendant coupling patterns in the ^{207}Pb and ^{119}Sn NMR spectra of the redistribution solutions. Mass spectrometric investigations revealed M_2 and M_3 units which confirmed the conclusions from the NMR examinations, and further, they showed signals assigned to M_4 units. On the basis of the appearance of the latter and the intermediate equivalent interceptable in the synthesis step (**6** in Scheme II), a unit similar to the intermediate (capable to reorganize) was assumed to be active in the exchange process as well. A possible route leading to the formation of the redistribution species observed in these exchange experiments is pictured in Scheme III.

At first, constant nucleophilic attacks of $>$M–S groups at tetrahedral R_2MS_2 systems (**8**) take place, creating the trigonal-bipyramidal adduct **9** in equilibrium with the starting substances. These attacks occur quickly, and because of the greater electrophilic behavior of the lead systems they occur more rapidly for the lead than for the corresponding tin systems. The sulfur atoms simultaneously carry out further nucleophilic attacks at the heavy-metal centers, resulting in the tetramer **10**, which possesses a ladderlike structure comparable to the intermediate **6** of the synthesis process. This step was considered to be

Scheme III

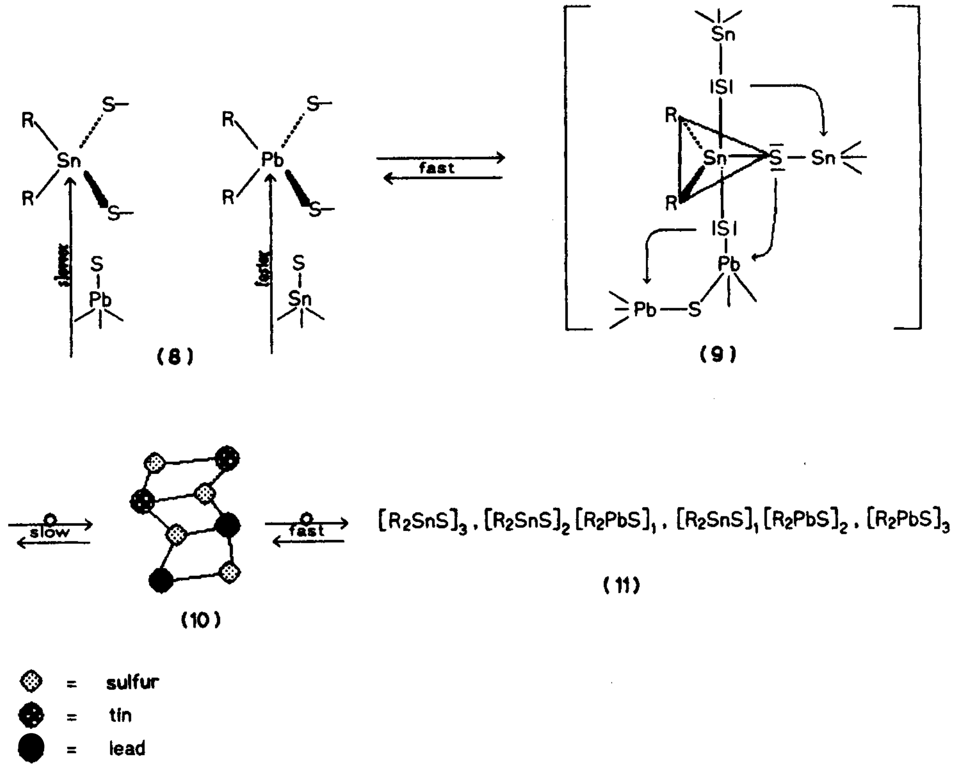

rate determining. The nucleophilic attacks of the sulfur atoms are promoted or restricted more or less by the different organic substituents bonded to the heavy-metal central atoms. This explains the retardation of the redistributions observed in systems when (oTol)$_2$S groupings are involved. Since the ladderlike tetramer 10 possesses both five-coordinate and four-coordinate Pb/Sn, of which the four-coordinate site is still electrophilic, further attacks occur, causing a rapid decay to yield the redistribution products 11. Although the lifetime of 10 was too short to allow it to be identified by NMR measurements, its steady-state concentration was high enough to be detected by FD mass spectrometry. In the steady state constant exchanges between the products 11 occur, each time involving 10. It is possible that for 10 "cubane-analogous" structures similar to those described by Molloy[12] and Harrison[13] are involved.

Experimental Section

Syntheses. Diorganometal^{IV}–sulfur heterocycles were synthesized according to well-known procedures[1,8,14–20] using difunctionalized metal diorganyls and hydrogen sulfide gas as reactants. However, some details were changed. Thus, using dry toluene as the reaction medium and triethylamine as an auxiliary base to intercept the hydrogenhalogenic acid formed, the base was not added in full amount to the solution of the applied diorganometal dihalogenide, but it was added dropwise simultaneously with hydrogen sulfide in order to ensure that the solution remained slightly acidic during the course of the reaction.

Table VI. Crystallographic Data for $Sn_4(cHex)_8Cl_2O_2(SH)_2$ and Structure Determination Details

Crystal Data (Mo Kα_1, λ = 0.709 26 Å)	
formula, M_r	$C_{48}H_{90}Cl_2O_2S_2Sn_4$, 1309.04
cryst habit	flat needle (cross-section with six faces)
face indices[a]	{001} (0.020 mm), {101} (0.050 mm), {010} (0.10 mm)
cryst color	colorless
cryst syst, space group	triclinic, $P\bar{1}$ (No. 2)
unit cell dimens (before intensity data collecn)[b]	
a (Å), α (deg)	11.718(5), 81.88(1)
b (Å), β (deg)	12.236(1), 87.71(3)
c (Å), γ (deg)	20.310(6), 75.64(1)
least-squares fit	75 rflns, θ = 14–17°
packing: V (Å^3), Z, $F(000)$ (e)	2793(2), 2 indep centrosymmetric molecules, 1320
D_{calcd}, D_{exptl} (g cm^{-3})	1.557, 1.531
Intensity Data Collection (Mo Kα, λ = 0.710 69 Å, Graphite Monochromator, $\omega/2\theta$ Scan)	
temp (°C), θ range (deg), $(\sin\theta)_{max}/\lambda$ (Å^{-1})	23, 1.5–26.0, 0.617
range of hkl	+14, ±16, ±26
ref rflns	3, every 20 000 s
loss of intensity (%) (time (days)), correcn	60 (22), spline
no. of rflns: measd, indep (int R)	12 333, 11 685 (0.0203)
no. of rflns used, limit	4151 with $I > 2\sigma(I)$
μ, abs correcn (cm^{-1})	18.18, numerical by face indices
range of transmissn	0.9298–0.8270
Refinement	
choice of thermal params	Sn, Cl, O, S anisotropic; C isotropic; no H considered
var, ratio reflns/var, last shifts	285, 14.6, <0.03σ
final R, R_w	0.0911, 0.1141
weight scheme w^{-1}	$\sigma^2(F) + 0.002643F^2$
final diff Fourier max(e Å^{-3})	1.4, inside the Sn(O,SH)Sn ring

[a] Distances from a common origin inside the crystal. [b] The unit cell expands during the data collection by about 1.5% (data after the measurement: a, b, c = 11.779(8), 12.262(2), 20.42(1) Å, α, β, γ = 81.79(2), 87.27(6), 75.85(2)°, V = 2830(4) Å^3, 86 reflections, θ = 14–17°).

---

(12) Molloy, K. *Adv. Organomet. Chem.* **1991**, *33*, 171.

(13) Harrison, P. G. *Chemistry of Tin*; Blackie & Son: Glasgow, London, 1989.

(14) Schmidt, B. M. Dissertation, Mainz, Germany, 1989.

(15) Ingham, R. K.; Rosenberg, S. D.; Gilman, H. *Chem. Rev.* **1960**, *60*, 459.

(16) *Gmelin Handbook of Inorganic Chemistry*; Springer-Verlag: Berlin, 1981; Organotin Compounds Part 1, p 2.

(17) Grüttner, G. *Ber. Dtsch. Chem. Ges.* **1914**, *47*, 3257.

(18) Kocheschkov, K. A.; Nadj, M. M. *Chem. Abstr.* **1935**, *29*, 3660.

(19) Berwe, H.; Haas, A. *Chem. Ber.* **1987**, *120*, 1175.

(20) Puff, H.; Bertram, G.; Ebeling, B.; Franken, M.; Gattermayer, R.; Hundt, R.; Schuh, W.; Zimmer, R. *J. Organomet. Chem.* **1989**, *379*(3), 235.

Table VII. Fractional Atomic Coordinates and Equivalent Isotropic Thermal Parameters for $Sn_4(cHex)_8Cl_2O_2(SH)_2$ (Triclinic, $P\bar{1}$; Esd's in Parentheses)

	molecule 1					molecule 2				
group[a]	atom	*x/a*	*y/b*	*z/c*	*U*(eq),[b] Å^2	atom	*x/a*	*y/b*	*z/c*	*U*(eq),[b] Å^2
core										
Sn1	Sn(1)	1.0596(1)	0.4627(1)	0.07577(8)	0.043(1)	Sn(3)	0.5709(1)	−0.0183(1)	0.57204(8)	0.047(1)
Sn2	Sn(2)	0.7491(1)	0.4764(1)	0.07308(9)	0.051(1)	Sn(4)	0.2596(1)	0.0921(1)	0.58551(9)	0.056(1)
SH	S(1)[c]	0.9150(6)	0.4247(5)	0.1762(3)	0.055(4)	S(2)[c]	0.4428(7)	0.0375(5)	0.6792(3)	0.059(4)
Cl	Cl(1)[c]	0.6579(6)	0.5305(6)	−0.0365(3)	0.069(5)	Cl(2)[c]	0.1445(7)	0.1218(7)	0.4849(4)	0.082(5)
O	O(1)	1.0992(15)	0.5087(14)	−0.0272(12)	0.091(15)	O(2)	0.5945(13)	−0.0381(11)	0.4686(8)	0.053(10)
cHex1	C(11)	1.1505(22)	0.2856(19)	0.0828(11)	0.049(6)*	C(31)	0.6518(24)	0.1194(21)	0.5712(12)	0.057(7)*
	C(12)	1.2272(27)	0.2421(24)	0.1437(14)	0.072(8)*	C(32)	0.5677(28)	0.2362(24)	0.5650(14)	0.074(8)*
	C(13)	1.2962(32)	0.1192(29)	0.1425(17)	0.097(11)*	C(33)	0.6317(33)	0.3380(30)	0.5526(18)	0.101(11)*
	C(14)	1.2053(31)	0.0435(28)	0.1396(16)	0.090(10)*	C(34)	0.7189(34)	0.3173(31)	0.6152(18)	0.104(11)*
	C(15)	1.1368(28)	0.0819(26)	0.0764(15)	0.080(9)*	C(35)	0.8073(35)	0.2014(33)	0.6203(19)	0.112(12)*
	C(16)	1.0562(27)	0.2175(24)	0.0759(14)	0.073(8)*	C(36)	0.7318(27)	0.1038(24)	0.6312(14)	0.073(8)*
cHex2	C(17)	1.0822(21)	0.6195(18)	0.1052(11)	0.042(6)*	C(37)	0.6138(25)	−0.1958(22)	0.6063(13)	0.061(7)*
	C(18)	1.1550(27)	0.5915(25)	0.1709(14)	0.074(8)*	C(38)	0.7041(28)	−0.2255(25)	0.6665(14)	0.076(9)*
	C(19)	1.1716(31)	0.7092(28)	0.1872(16)	0.092(10)*	C(39)	0.7409(30)	−0.3633(28)	0.6865(16)	0.088(10)*
	C(110)	1.0548(29)	0.7945(27)	0.1943(15)	0.086(10)*	C(310)	0.6330(30)	−0.4014(27)	0.7087(16)	0.086(9)*
	C(111)	0.9781(31)	0.8154(28)	0.1284(16)	0.091(10)*	C(311)	0.5446(30)	−0.3769(27)	0.6517(16)	0.090(10)*
	C(112)	0.9590(26)	0.7022(23)	0.1142(13)	0.065(7)*	C(312)	0.5071(26)	−0.2406(24)	0.6277(14)	0.070(8)*
cHex3	C(21)	0.7298(26)	0.3046(23)	0.0960(14)	0.066(8)*	C(41)[d]	0.2324(27)	0.2666(23)	0.6049(14)	0.068(8)*
	C(22)	0.6229(35)	0.3032(33)	0.1420(19)	0.110(12)*	C(42)	0.1296(46)	0.2849(44)	0.6514(26)	0.163(19)*
	C(23)	0.6035(35)	0.1861(33)	0.1650(19)	0.111(12)*	C(43)	0.0900(47)	0.4224(48)	0.6682(27)	0.169(19)*
	C(24)	0.6086(38)	0.1254(34)	0.1041(21)	0.122(13)*	C(44)	0.0690(44)	0.4917(40)	0.6036(25)	0.146(16)*
	C(25)	0.7051(34)	0.1293(31)	0.0512(19)	0.106(12)*	C(45)	0.1772(46)	0.4840(42)	0.5636(24)	0.148(17)*
	C(26)	0.7225(31)	0.2477(29)	0.0338(17)	0.091(10)*	C(46)	0.2067(40)	0.3599(39)	0.5413(21)	0.135(15)*
cHex4	C(27)[d]	0.6558(29)	0.6233(26)	0.1170(16)	0.080(9)*	C(47)[d]	0.2035(28)	−0.0512(25)	0.6419(15)	0.075(8)*
	C(28)	0.6042(33)	0.7192(31)	0.0733(18)	0.102(11)*	C(48)	0.1406(47)	−0.1069(45)	0.5932(25)	0.166(19)*
	C(29)	0.5282(44)	0.8144(41)	0.1141(26)	0.152(17)*	C(49)	0.1149(48)	−0.2197(44)	0.6439(26)	0.162(18)*
	C(210)	0.4910(49)	0.7892(46)	0.1804(28)	0.163(19)*	C(410)	0.0265(44)	−0.1668(41)	0.6913(24)	0.145(16)*
	C(211)	0.5397(39)	0.6934(38)	0.2249(22)	0.129(14)*	C(411)	0.0712(36)	−0.1063(34)	0.7362(20)	0.115(13)*
	C(212)	0.6244(43)	0.5904(41)	0.1851(24)	0.149(17)*	C(412)	0.1172(35)	−0.0062(32)	0.6920(19)	0.110(12)*

[a] Labeling as given in Figure 1 and used in Table II. [b] *U*(eq) = one-third of the trace of the isotropic U(*ij*) tensor; asterisks indicate isotropic *U* values. [c] The possibility of a mutual interchange between S and Cl cannot be fully excluded. [d] These three cHex groups are slightly disordered.

In this way, the occurrence of white flakes, which could be observed when the full amount of the auxiliary base was added prior to the sulfide, could be avoided. When organolead compounds were starting materials, hydrogen sulfide was placed over the stirred reaction solution in a balloon to slow the reaction, because if it was bubbled directly into the solution, black PbS precipitated at once. Triethylamine–hydrochloride separates from the toluene while the product remains in solution.

Likewise, ethanol can be used as solvent, keeping constant all other working conditions which cause the product to precipitate while the $NEt_3{\cdot}HX$ remains dissolved. However, in the synthesis a delay of the reaction occurred when diorganotin dichlorides were the starting materials. The expected precipitation of the heterocyclic products did not take place as soon as auxiliary base NEt_3 was added; instead, the reaction mixture remained a clear solution for several minutes and then suddenly the product precipitated, almost quantitatively, within a few seconds.

$Sn_4(cHex)_8Cl_2O_2(SH)_2$ was obtained from the reaction of $(cHex)_2SnCl_2$ and H_2S in moist toluene under slightly basic conditions. First 1 g (23.25 mmol) of triethylamine was poured into a solution of 1.6 g (4.5 mmol) of the dichloride in toluene to guarantee basic conditions; then, an H_2S atmosphere was applied to the solution by fitting a hydrogen sulfide filled balloon to the reaction flask. The mixture was stirred rapidly for 24 h at room temperature and then separated from the precipitated $NEt_3{\cdot}HCl$. Dissolved hydrogen sulfide was removed by the application of a vacuum to the filtrate, which then was stored under a petroleum ether (30–70 °C) atmosphere in the dark at room temperature for several weeks. The yellowish liquid was decanted from the precipitated white solid, which then was dissolved again in chloroform or benzene. These solutions were also submitted to petroleum ether atmospheres. In both cases, after several weeks, a few fragile white crystals had grown. The yield was not determined. According to X-ray structure analysis the crystals from the two processes are identical in structure. Anal. Calcd for $C_{48}H_{90}Cl_2O_2S_2Sn_4$ (M_r = 1309.04): C, 44.0; H, 6.9; Cl, 5.4; S, 4.9. Found (impure crystals): C, 44.4, H, 6.8; Cl, 5.9; S, 2.0. The deviation of S contents can be explained by partial incorporation of oxygen instead of sulfur in non-single-crystal material (see Syntheses and Synthetic Intermediates in the Discussion). EI mass spectrometry (single crystal; given here are the highest signals (*m/e*) of the patterns observed and the assigned fragments (highest peak from computer simulation in parentheses)): 408, $(cHex)Sn_2ClO(SH)$ (405); 572, $(cHex)_3Sn_2ClO(SH)$ (571); 654, $(cHex)_4Sn_2ClO(SH)$ (654); 738, $(cHex)_3Sn_3ClO_2(SH)_2$ (740); 821, $(cHex)_4Sn_3ClO_2(SH)_2$ (823). The observed patterns correspond to the simulated ones; however, for the cases mentioned above similar isotopic patterns occur when Cl is replaced by SH. Slightly better agreement is obtained by referring to both the pattern and the highest signal within this pattern if the assignment given is assumed to be correct.

Crystal Structure Determination of $Sn_4(cHex)_8Cl_2O_2(SH)_2$. The crystalline material from both workup procedures of $Sn_4(cHex)_8Cl_2O_2(SH)_2$ is isomorphous according to Weissenberg exposures and diffractometer indexings of several single crystals. For two crystals—one obtained from benzene and the other from chloroform/petroleum ether—full intensity data collections were made. The results from both measurements are identical within the esd's; the data of the crystal from benzene are slightly better and are given in the tables. Both crystals decomposed slowly during the data collection; simultaneously their unit cells expanded by about 1.5%. This expansion causes somewhat imprecise atom positions and limits the accuracy of the structure determination severely. For the geometrical calculations (Table II) the unit cell dimensions before data collection were used.

Crystal data as well as details of intensity data collection and refinement are given in Table VI. The density was obtained by flotation in aqueous sodium polytungstate solution. In comparison with the calculated values, slightly lower numbers were found. This can be explained by the same factors which cause the above-mentioned deviation in the elementary analysis. The crystal was fixed with glue and sealed in a glass capillary. Integrated intensities were measured on a CAD4 diffractometer (Enraf-Nonius).

The structure was solved by a Patterson synthesis (Sn atoms) and completed by Fourier (Cl and S atoms) and weighted difference Fourier synthesis (O and C atoms). The refinement resulted in a good convergence and in even variances. Besides several locally written routines, local versions of Shelx-76 and Shelx-86 were used for the calculations and Pluto-78 was used for the creation of Figure 1 (VAX cluster at Zentrum für Datenverarbeitung, Universität Mainz). Table VII contains the final parameters.

NMR Experiments. The starting materials for the redistribution experiments were purified by recrystallization before NMR experiments. For each exchange experiment, one tin and one lead heterocycle were dissolved at room temperature in $CDCl_3$ in concentrations of about 5.5×10^{-2} M (100–300 mg/3 mL) in 10-mm-diameter NMR studies. Immediately afterward, these solutions were submitted to ^{119}Sn and ^{207}Pb NMR spectroscopy. While the tin heterocycles are stable in solution, the lead heterocycles degrade slowly, forming a black precipitate thought to be lead and lead sulfide. However, degradation occurred too slowly to influence the NMR studies. The measurements were conducted at about 300 K under the influence of ^{1}H decoupling and in the FT mode. The digital resolution was 0.5 Hz. Equipment for NMR measurements: Bruker WP 80-DS. Measuring frequencies: ^{13}C measurements, 20.15 MHz; ^{207}Pb measurements, 16.74 MHz; ^{119}Sn measurements, 29.88 MHz.

Mass Spectrometric Experiments. After the NMR experiments had been conducted, the solutions were filtered and immediately examined by means of FD mass spectrometry. Equipment for mass spectrometric measurements: Finigan MAT 8230, field desorption potential: 6 kV. Acceleration potential: 3 kV.

Acknowledgment. We thank the Deutsche Forschungsgemeinschaft, Bad Godesberg, Germany, and the Fonds der Chemischen Industrie, Frankfurt/Main, Germany, for financial support.

Supplementary Material Available: Tables listing anisotropic thermal parameters, complete bond lengths and angles, torsion angles, and mass spectroscopic results in detail (10 pages). Ordering information is given on any current masthead page.

OM9303459